EASR

Engineering and Applied Science Research

https://www.tci-thaijo.org/index.php/easr/index

Published by the Faculty of Engineering, Khon Kaen University, Thailand

Stress-strain relationships of spirally confined instant concrete under axial compression

Mohammad Ghozi*[1)], Anik Budiati[1)], Bambang Sabariman[2)], Tavio[3)] and Slamet Widodo[4)]

[1)]Department of Civil Engineering, Universitas Bhayangkara Surabaya, 60231, Indonesia
[2)]Department of Civil Engineering, Universitas Negeri Surabaya, 60231, Indonesia
[3)]Department of Civil Engineering, Institut Teknologi Sepuluh Nopember, Surabaya, 60111, Indonesia
[4)]Department of Civil Engineering and Planning, Universitas Negeri Yogyakarta, 55281, Indonesia

Received 13 November 2024
Revised 13 February 2025
Accepted 18 February 2025

Abstract

Project activities require the strength of concrete to reach 100% at an age less than 28 days. Many manufacturers have created concrete with a strength that reaches 100% at an age less than 28 days; this product is called instant concrete. This instant concrete can be designed to attain 100% concrete strength at the ages of 7, 14, and 21 days. However, concrete is not only required to be strong; it must also be ductile. Ductility is usually measured after the concrete reaches its peak load phase, namely in inelastic conditions. Square or spiral stirrups can be used for concrete confinement to improve ductility. Spirals are a better confining system than square stirrups. The evidence for this can be seen from the relationship between concrete stress and strain. The concrete stress-strain relationship is necessary as a basis for reinforced concrete design assumptions. However, for instant concrete with a certain age, it is necessary to develop its specific stress-strain relationship model. Thus, this study aims to develop a stress-strain relationship model that can be used as a basis for assumptions in analysing confined concrete structural members. This study measured the concrete strength f'_c at the ages of 7, 14, 21, and 28 days, and on average it reached the target f'_c value; the stress-strain relationship tends to fit the Kent-Park model. Therefore, the design of reinforced concrete structural members for the ages of 7, 14, and 21 days can use the proposed stress-strain relationship model.

Keywords: Concrete age, Confinement, Inelastic state, Spiral, Stress-strain relationship model

1. Introduction

The characteristic compressive strength of concrete is generally achieved and measured at the age of 28 days. This age is the normal age obtained from the concrete's compressive strength test. The measurement is carried out using concrete cylinder compressive loading [1-4]. The basic concrete materials are normally sand, gravel, cement, and water, and they sometimes include additives [5-12]. The use of additives is meant to improve workability, reduce hydration heat, increase the concrete compressive strength and ductility, reduce shrinkage, and also accelerate the achievement of the required concrete strength before an age of 28 days is reached, among others. However, the crucial factor that needs to be observed is the concrete stress-strain (σ_c-ε_c) relationship, because the σ_c-ε_c relationship is used as the basis for concrete design [13]. Several normal and high-strength concrete stress-strain relationships, including those of confined and unconfined concrete [14-31] and fibre concrete, have been widely studied, and their characteristics vary widely [32-38]. If the design basis is used, the equation used is different. Thus, it is necessary to determine the σ_c-ε_c relationship of concrete before it reaches an age of 28 days, since currently many concrete work specifications require concrete to reach 100% strength before an age of 28 days, so that the assumption of the σ_c-ε_c relationship becomes crucial for design applications.

Along with the requirements and developments in concrete construction, concrete technology, and concrete materials, instant concrete (IC) has now been widely developed and used [39]. IC is intended to accelerate the achievement of the maximum concrete compressive strength before the age of 28 days; it can even be achieved in just a few hours [40]. Research on the effect of the concrete age on σ_c-ε_c relationships has been conducted, and the results are satisfactory [41]. However, concrete is not only required to be strong; it is also required to be ductile. This ductility is obtained after it passes through the maximum concrete strength phase, the condition beyond the maximum compressive strength (inelastic region), which can be used to categorise concrete as brittle or ductile concrete [15, 16]. This category is determined based on the stress-strain (σ_c-ε_c) relationship of concrete, meaning that the σ_c-ε_c relationship is an important parameter to consider when a ductile form of concrete is required.

The characteristics of the σ_c-ε_c relationship, both confined and unconfined, must be known because this relationship can be used to derive mathematical equations for modelling the behaviour of confined concrete as an input for the analysis and design of reinforced concrete [13]. Several of the studies mentioned above proposed σ_c-ε_c relationships in elastic and inelastic conditions. Hence, according to the needs of the design of reinforced concrete structures, an appropriate σ_c-ε_c relationship is necessary. Likewise, the σ_c-ε_c relationship model of IC also needs to be obtained when it is applied in structural concrete design. The correct σ_c-ε_c relationship model must be used to obtain better design results.

*Corresponding author.
Email address: mghozi@ubhara.ac.id
doi: 10.14456/easr.2025.17

2. Methodology

This study examines variations in the effect of the concrete age on concrete stress-strain relationships, namely concrete stress-strain relationships at the ages of 7, 14, 21, and 28 days. The concrete compressive strength (σ_c) at each age is expected to be similar. In addition to the compressive strength of the test specimens, the concrete strain (ε_c) was also investigated. In this study, observations were carried out to obtain both σ_c and ε_c, starting from initial loading and continuing until the test specimen failed. The graphical representations in terms of σ_c-ε_c curves were then plotted from the σ_c-ε_c test data. The research flowchart can be seen in Figure 1.

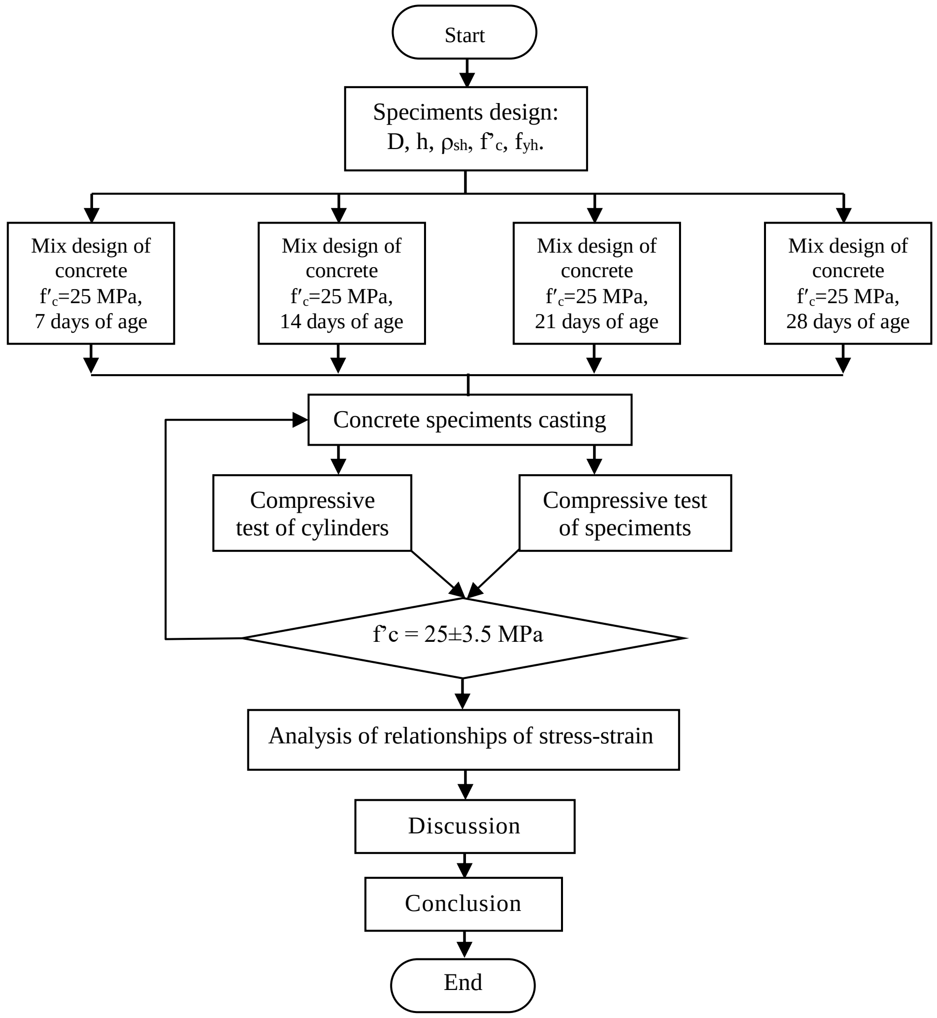

Figure 1 Research flowchart

2.1 Concrete stress-strain model (σ_c-ε_c)

The stress-strain relationship uses the Kent-Park model [15] (Figure 2) because it is used in several previous studies, and the formulation of this model is as follows:

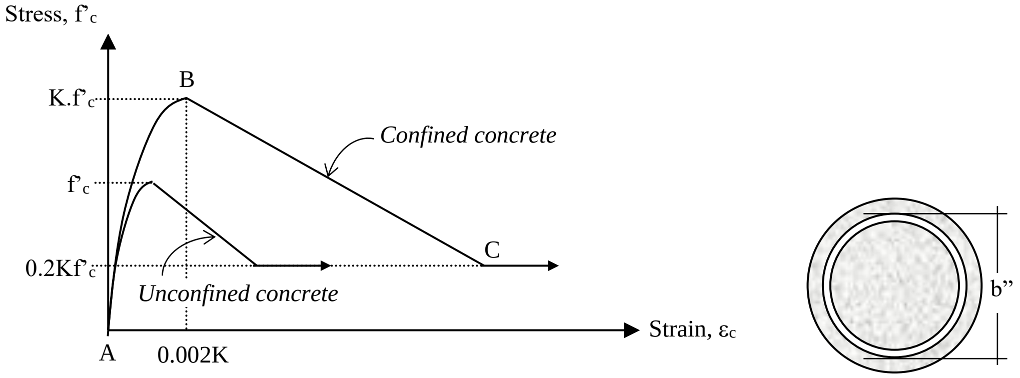

Figure 2 Stress-strain relationship of modified Kent-Park model and dimension of b" [15]

Region AB: $\varepsilon_c \leq 0.002K$:

$$f_c = Kf'_c\left[\frac{2\varepsilon_c}{0.002K} - \left(\frac{\varepsilon_c}{0.002K}\right)^2\right]. \tag{1}$$

Region BC: $\varepsilon_c > 0.002K$:

$$f_c = Kf'_c\,[\,1 - Z_m\,(\varepsilon_c - 0.002K)\,], \tag{2}$$

but not less than $0.2Kf'_c$:

$$K = 1.25\left(1 + \frac{\rho_s f_{yh}}{f'_c}\right), \tag{3}$$

$$Z_m = \frac{0.625}{\left[\frac{3+0.29f'_c}{145f'_c-1000}\right] + \frac{3}{4}\rho_s\sqrt{\frac{b"}{s_h}} - 0.002K}, \tag{4}$$

where

- Z_m = the concrete confinement value of the modified Kent-Park model;
- K = the multiplication factor;
- ρ_s = the volumetric ratio of the spiral to the confined concrete core measured from outer point to outer point of the spiral;
- s_h = the spacing from centre to centre of the spiral (mm);
- f_{yh} = the yield strength of the spiral (MPa);
- f'_c = the concrete compressive strength (MPa);
- b" = the cross-sectional dimension of the confined concrete core measured from outer point to outer point of the spiral (mm).

The value of Z_m is very important in defining the influence of confinement. Using the value of Z_m, the value of s_h (the spiral spacing) can be found. Likewise, if the spiral spacing is known, the value of Z_m can be determined. On the moment-ductility curve, good confinement can be achieved with a low value of Z_m. A low value of Z_m can be obtained by increasing the value of ρ_s. The greater the value of ρ_s, the better the confinement, and the lower the value of Z_m, the better the curvature ductility of the confined concrete.

2.2 Materials and specimens

The concrete used in this research is normal-strength concrete with $f'_{c\text{-target}}$ = 25 MPa (see Table 1). An IC product was used. The reinforcing steel used had a diameter of 8 mm for the spiral. Concrete reinforcement involved a steel spiral with the spacing s_h = 37 mm. The details of the test specimens are listed in Table 2.

2.3 Experimental programme

Based on Formulas 1–4 and Tables 1 and 2, the test specimens of IC were made and confined with the steel spiral (see Figure 3). These test specimens (Figure 3) were divided into four groups according to the ages of instant concrete used, namely 7, 14, 21, and 28 days. After the casting process was completed, the wet curing of concrete was then carried out until one day before the testing day (lifted out of water containment). After air drying for a day, capping was applied. Compression tests were then conducted using a universal testing machine (UTM) with a capacity of 2000 kN. By recording the load/force P (kN) and Δ (mm), the σ_c-ε_c relationship can be obtained. In addition, visual observations were also made on the cracks of the test specimens during the testing process.

Table 1 Mix design for a volume of 1 m^3 (SSD (Saturated Surface Dry) condition) concrete with f'_c of 25 MPa [39]

No.	Materials	Value	Description
1.	Max. aggregate size (mm)	15	
2.	Slump (cm)	12±2	
3.	W/C (Water/Cement) ratio	0.35	Age of 7 days
		0.40	Age of 14 days
		0.45	Age of 21 days
		0.50	Age of 28 days
4.	Cement content (kg/m^3)	490–500	Age of 7 days
		445–455	Age of 14 days
		400–410	Age of 21 days
		380–390	Age of 28 days
5.	Admixture (kg)	1–1.5	
6.	Water estimation (ltr/m^3)	170–190	
7.	Coarse aggregate, 5–15 mm (kg/m^3)	911–919	Age of 7 days
		935–943	Age of 14 days
		957–969	Age of 21 days
		967–979	Age of 28 days
8.	Fine aggregate, <5 mm (kg/m^3)	706–714	Age of 7 days
		726–732	Age of 14 days
		742–754	Age of 21 days
		751–759	Age of 28 days

Table 2 Details of test specimens

No.	Specimen ID	Age (days)	ϕ (mm)	L (mm)	Spiral		f_{yh} (MPa)	$f'_{c\text{-average}}$ (MPa)	Z_m
					ϕ (mm)	s_h (mm)			
1.	$S_{7.1}$	7	150	300	8	37	327.80	22.437	17.390
2.	$S_{7.2}$	7	150	300	8	37	327.80	22.437	17.390
3.	$S_{7.3}$	7	150	300	8	37	327.80	22.437	17.390
4.	$S_{14.1}$	14	150	300	8	37	327.80	23.921	17.019
5.	$S_{14.2}$	14	150	300	8	37	327.80	23.921	17.019
6.	$S_{14.3}$	14	150	300	8	37	327.80	23.921	17.019
7.	$S_{21.1}$	21	150	300	8	37	327.80	25.053	16.763
8.	$S_{21.2}$	21	150	300	8	37	327.80	25.053	16.763
9.	$S_{21.3}$	21	150	300	8	37	327.80	25.053	16.763
10.	$S_{28.1}$	28	150	300	8	37	327.80	24.594	16.864
11.	$S_{28.2}$	28	150	300	8	37	327.80	24.594	16.864
12.	$S_{28.3}$	28	150	300	8	37	327.80	24.594	16.864

Figure 3 Details of spiral with ϕ = 8 and s_h = 37 mm (the specimens had no longitudinal or main steel bars) and ready-to-test capped concrete specimens

2.4 Test setup

During testing, several data-recording instruments were connected to a recorder unit, which was then connected directly to a computer unit. The actual test setup is shown in Figure 4.

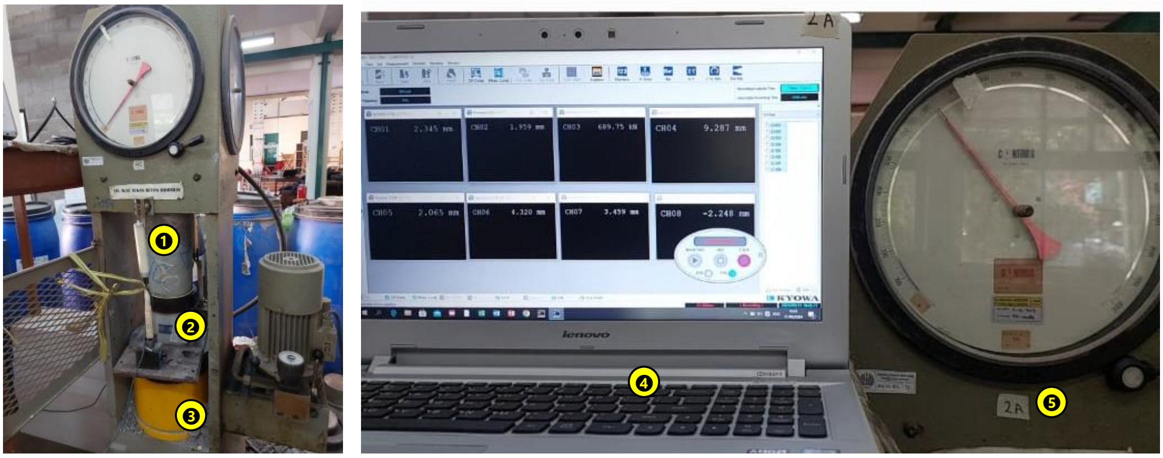

Figure 4 Actual test setup: ❶ LVDT (Linear Variable Displacement Transducer) vertical, cap. 50 mm; ❷ single-acting load cell, cap. 1 MN; ❸ single-acting hydraulic jack, cap. 200 kN; ❹ computer; ❺ manometer

3. Results and discussion

3.1 Concrete compression test results

To obtain the actual concrete strengths, compressive tests were conducted using three concrete cylinders with a diameter of 150 mm and a height of 300 mm (Table 3). The casting of the concrete cylinders was performed at the same time as the casting of test specimens. After the concrete cylinders were 7, 14, 21, and 28 days old, compressive tests were carried out. The results of the compressive tests for each age are given in Table 3.

Table 3 Compressive strength of concrete at 7, 14, 21, and 28 days of age

No.	Specimen	Compressive strength (MPa)	Deviation from f'_c = 25 ± 3.5 MPa [42]	Average compressive strength (MPa)	Average deviation from f'_c = 25 ± 3.5 MPa [42]
1.	C_{7-1}	23.674	-1.326		
2.	C_{7-2}	21.550	-3.45		
3.	C_{7-3}	22.087	-2.913	22.437	-2.563
4.	C_{14-1}	21.798	-3.202		
5.	C_{14-2}	23.213	-1.787		
6.	C_{14-3}	26.752	1.752	23.921	-1.079
7.	C_{21-1}	25.477	0.477		
8.	C_{21-2}	26.115	1.115		
9.	C_{21-3}	23.567	-1.433	25.053	0.053
10.	C_{28-1}	25.478	0.478		
11.	C_{28-2}	24.736	-0.264		
12.	C_{28-3}	23.567	-1.433	24.594	-0.406

Note: For C_{n-i}, C = cylinder, n = concrete age, and i = concrete sample #.

3.2 Reinforcing steel tensile test results

Reinforcing steel bars with a diameter of 8 mm were used for confinement in the concrete specimens in the form of a spiral. Tensile tests of steel bars were carried out using a 2000-kN UTM (Figure 5), and the yield strengths (f_{yh}) of the steel bars (around 327 MPa) obtained from the tests are also given in Table 4 for each sample. The tensile strengths (f_{y-max}) of the steel bars (around 471 MPa) are also given in Table 4, along with the ratios of the tensile to yield strengths (around 1.45) and the maximum elongations (around 26.23%) of the steel bars. The values in Table 4 are essential for the design of reinforced concrete structural members.

Figure 5 Tensile test of steel bars with UTM cap. 2000 kN

Table 4 Specification of ϕ = 8 mm steel bars for transverse reinforcement (stirrups)

No.	Sample ID	D_{ef} (mm)	f_{yh} (MPa)	f_{y-max} (MPa)	Ratio (f_{y-max}/f_{yh})	Elongation (%)
1.	St.8-1	7.87	325.88	475.06	1.46	25.60
2.	St.8-2	7.87	323.68	460.84	1.42	27.50
3.	St.8-3	7.91	328.73	479.86	1.46	25.60
	Average	7.88	327.80	471.92	1.45	26.23

3.3 Test Results of specimens

After the test specimens reached ages of 7, 14, 21, and 28 days, the compressive tests were carried out, as explained in the previous section. The test results were then used to create a graphical representation and further analysed. The test results in terms of stress-strain curves are presented in Figures 6–9, and the data values are summarised in Table 5.

Based on Figures 6–9, the σ_c-ε_c relationship of spirally confined concrete shows higher peak stresses, and the ductilities also increase compared to the σ_c-ε_c relationship of unconfined concrete. This indicates that the spirally confined concrete demonstrated ductile behaviour, which is indicated by its post-peak response, with a longer strain and a more slowly degrading slope.

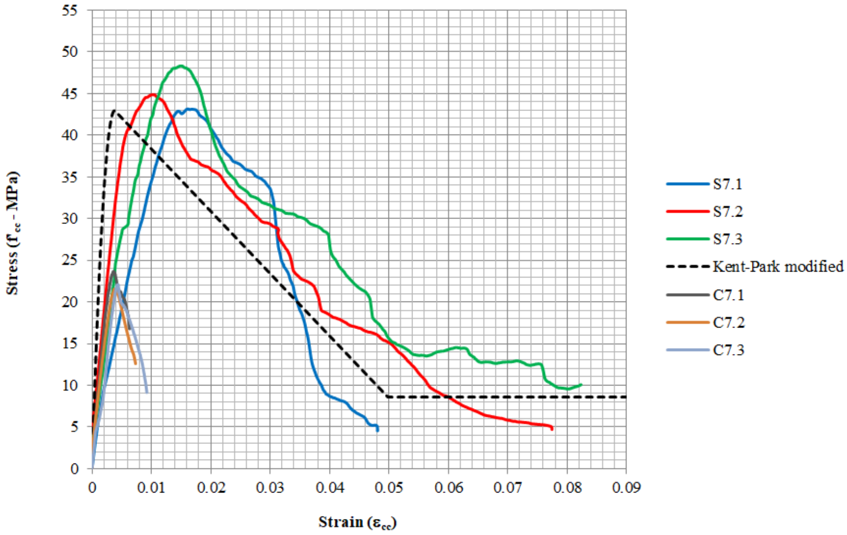

Figure 6 Strain-stress relationship of confined concrete at age of 7 days

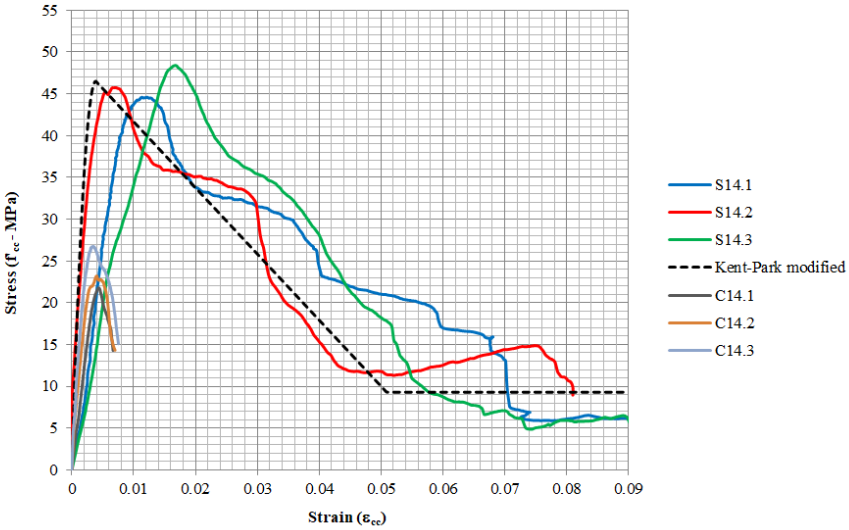

Figure 7 Strain-stress relationship of confined concrete at age of 14 days

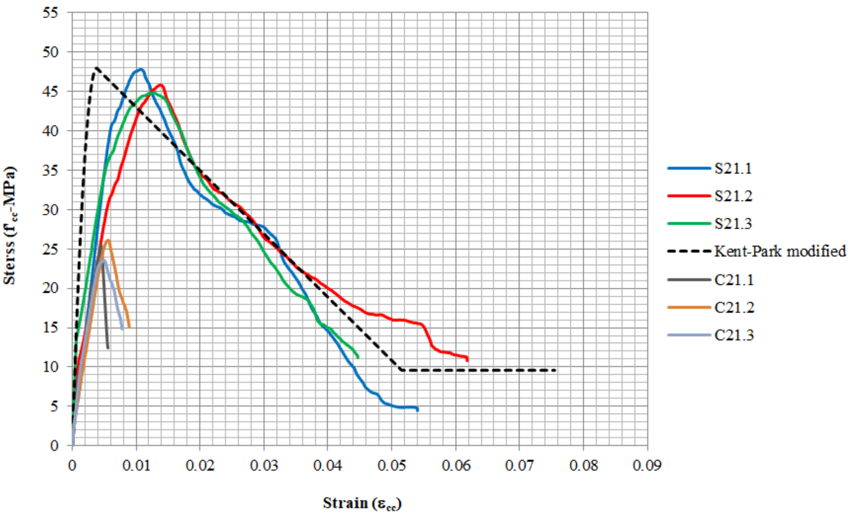

Figure 8 Strain-stress relationship of confined concrete at age of 21 days

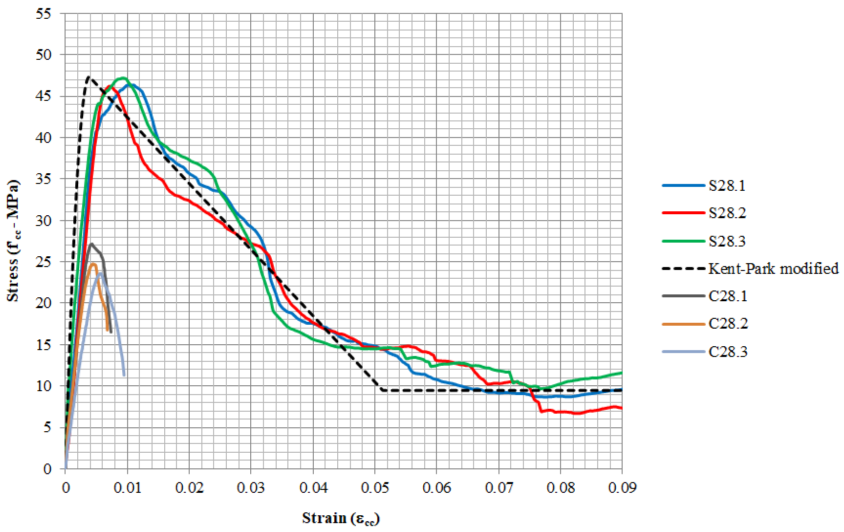

Figure 9 Strain-stress relationship of confined concrete at age of 28 days

Table 5 Stress and strain of confined concrete at ages of 7, 14, 21, and 28 days

No.	Specimen	Stress (f'_{cc}, MPa)	Strain (ε_{cc})
1.	$S_{7.1}$	43.134	0.01609
2.	$S_{7.2}$	44.856	0.01038
3.	$S_{7.3}$	48.309	0.01501
4.	KP_7	42.953	0.00382
5.	$S_{14.1}$	44.601	0.01222
6.	$S_{14.2}$	45.743	0.00704
7.	$S_{14.3}$	48.402	0.01682
8.	KP_{14}	46.511	0.00389
9.	$S_{21.1}$	47.801	0.01080
10.	$S_{21.2}$	45.812	0.01379
11.	$S_{21.3}$	44.821	0.01271
12.	KP_{21}	47.962	0.00383
13.	$S_{28.1}$	46.346	0.01093
14.	$S_{28.2}$	46.192	0.00715
15.	$S_{28.3}$	47.187	0.00925
16.	KP_{28}	47.352	0.00385

Note: KP indicates the stress and strain from the modified Kent-Park model.

Based on Table 3, it can be seen that the lowest actual compressive strength value is 21.550 MPa, and the highest value is 26.752 MPa; meanwhile, the lowest average value is 22.437 MPa, and the highest average value is 25.053 MPa. All of the above values can be categorised as being within the acceptable range of concrete strength, because the target f'_c range is 25 ± 3.5 MPa [42].

In addition, based on Figures 6–9 and Table 5, it can be seen that all test specimens with confinement experienced an increase in σ_c-ε_c compared to test specimens without confinement and almost the same level of achievement; the actual compressive strength (f'_{cc}) results ranged from 43.134 to 48.402 MPa. Regarding the age groups of test specimens, it can be seen that test specimens with an age of 7 days experienced an increase in σ_c-ε_c. Only the initial stiffness of the 7-day-group test specimens varied. For test specimens aged 14 days, the σ_c-ε_c results were not much different from those of the test specimens aged 7 days. Test specimens aged 21 days began to differ from test specimens aged 7 and 14 days, which had similar stiffness values. Meanwhile, in the group of test specimens aged 28 days, the initial stiffness and σ_c-ε_c began to overlap, and the post-inelastic σ_c-ε_c values began to overlap.

In general, this study does not need to propose a new equation, because the observed σ_c-ε_c behaviour tends to follow the pattern of the Kent-Park σ_c-ε_c model [15], especially for test specimens in the 28-day age group, although the initial stiffness is still less in accordance with the Kent-Park model. However, if the initial stiffness needs to be improved, then this can be done by introducing more of a spiral or more confinement [43], namely a greater diameter or a smaller pitch or spacing.

Based on the observations above, this study can be considered on the conservative side, meaning that the σ_c-ε_c relationship at the ages of 7, 14, and 21 days can still be used as the basis/assumption for structural concrete design, while the σ_c-ε_c relationship at 28 days of age can be used directly as the basis/assumption for structural concrete design.

4. Conclusion

From the study above, it can be concluded that the compressive strength values of test specimens from all age groups met the target compressive strength f'_c = 25 ± 3.5 MPa, while the stress-strain relationship of confined concrete at all ages tends to follow the Kent-Park model. Thus, if the structure is designed using IC aged 7, 14, and 21 days, then the stress-strain assumption can use the Kent-Park model for concrete. This model also shows that the spirally confined concrete demonstrated ductile behaviour, which is indicated by its post-peak response.

5. Acknowledgment

The authors would like to express their sincere gratitude for all the funding received from the 2024 PDP Research grant, under Universitas Bhayangkara Surabaya with contract no. 008/SP2H/PT/LL7/2024 and DRTPM-LLDIKTI with contract no. 109/E5/PG.02.00PL/2024.

6. References

[1] Indonesian National Standard. SNI 7656:2012. Procedures for selecting mixtures for normal concrete, heavy concrete and mass concrete. Jakarta: National Standardization Agency; 2012. (In Indonesian)
[2] Indonesian National Standard. SNI-03-2834-2000. Procedures for making normal concrete mixtures. Jakarta: National Standardization Agency; 2000. (In Indonesian)
[3] Indonesian National Standard. SNI 4810:2013. Procedures for making and curing concrete test specimens in the field. Jakarta: National Standardization Agency; 2013. (In Indonesian)
[4] ASTM. ASTM C31/C31M-09: Standard practice for making and curing concrete test specimens in the field. West Conshohocken: ASTM International; 2009.
[5] Rakhimova G, Slavcheva G, Aisanova M, Rakhimov M, Tkach E. The influence of a complex additive on the strength characteristics of concrete for road construction. Int J GEOMATE. 2023;25(110):243-50.
[6] Tuskaeva Z, Karyaev S. Influence of various additives on properties of concrete. E3S Web of Conf. 2020;164:14007.
[7] Gallegos-Villela RR, Larrea-Zambrano FD, Goyes-Lopez CE, Perez-Sanchez JF, Suarez-Dominguez EJ, Palacio-Perez A. Effect of natural additives on concrete mechanical properties. Cogent Eng. 2021;8(1):1870790.
[8] Bhatt HJ, Prajapati DP, Khalak AA, Patel MJ. Advancements in cement technology: a comprehensive review of additives and their impact on material properties. Int J Res Publ Rev. 2023;4(12):1105-12.
[9] Placzek G, Schwerdtner P. Concrete additive manufacturing in construction: integration based on component-related fabrication strategies. Buildings. 2023;13(7):1769.
[10] Belaid F. How does concrete and cement industry transformation contribute to mitigating climate change challenges?. Resour Conserv Recycl Adv. 2022;15:200084.
[11] Angst UM, Geiker M. Moisture in concrete and its influence on durability. Cement. 2023;14:100087.
[12] Shah, V. Performance evaluation of carbonated cement paste derived from hydrated Portland cement-based binders as supplementary cementitious material. Cement. 2024;15:100091.
[13] Pincheira JA, Parra-Montesinos GJ, Wang CK, Salmon CG. Reinforced concrete design. 9th ed. USA: Oxford University Press; 2021.
[14] Machmoed SP, Tavio, Raka IGP. Performance of square reinforced concrete columns confined with innovative confining system under axial compression. Int J GEOMATE. 2021;21(85):137-44.
[15] Scott BD, Park R, Priestley MJN. Stress-strain behavior of concrete confined by overlapping hoops at low and high strain rates. ACI J. 1982;79(1):13-27.
[16] Paulay T, Priestley MJN. Seismic design of reinforced concrete and masonry buildings. New York: John Wiley & Sons Inc; 1992.
[17] Sheikh SA, Uzumeri SM. Strength and ductility of tied concrete columns. J Struct Div. 1980;106(5):1079-1102.
[18] Pinto D, Tavio, Raka IGP. Axial compressive behavior of square concrete columns retrofitted with GFRP straps. Int J Civ Eng Technol. 2019;10(1):2388-400.
[19] Sheikh SA, Uzumeri SM. Analytical model for concrete confinement in tied columns. J Struct Div. 1982;108(12):2703-22.
[20] Sheikh SA, Toklucu MT. Reinforced concrete columns confined by circular spirals and hoops. ACI Struct J. 1993;90(5):542-53.
[21] Assa B, Nishiyama M, Watanabe F. New approach for modeling confined concrete. I: circular columns. J Struct Eng. 2001;127(7):743-50.
[22] Khatulistiani U, Tavio, Raka IGP. Influence of steel bars for external confinement on compressive strength of concrete. Int J GEOMATE. 2021;20(82):146-52.
[23] Legeron F, Paultre P. Uniaxial confinement model for normal and high-strength concrete columns. J Struct Eng. 2003;129(2):241-51.
[24] Samani AK, Attard MM. A stress-strain model for uniaxial and confined concrete under compression. Eng Struct. 2012;41:335-49.
[25] Razvi S, Saatcioglu M. Confinement model for high-strength concrete. J Struct Eng. 1999;125(3):281-9.
[26] Agustiar, Tavio, Raka IGP, Anggraini R. Behavior of concrete columns reinforced and confined by high-strength steel bars. Int J Civ Eng Technol. 2018;9(7):1249-57.
[27] Seong DJ, Kim TH, Oh MS, Shin HM. Inelastic performance of high-strength concrete bridge columns under earthquake loads. J Adv Concr Technol. 2011; 9(2):205-20.
[28] Cusson D, Paultre P. Stress-strain relationship for confined high-strength concrete. J Struct Eng. 1995;121(3):468-77.
[29] Elwood KJ, Maffei J, Riederer KA, Telleen K. Improving column confinement-part 2: proposed new provisions for the ACI 318 building code. Concr Int. 2009;31(12):41-8.
[30] Honestyo A, Tavio, Ardhyananta H. Axial compressive behavior of bubble-size plastic straw waste FRP-confined circular concrete. Int J Eng Appl. 2023;11(2):73-80.
[31] Machmoed SP, Tavio, Raka IGP. Potential of new innovative confinement for square reinforced concrete columns. J Phys: Conf Ser. 2020;1469:012027.
[32] Oliveira LA, Borges VES, Danin AR, Machado DVR, Araújo DL, El Debs MK, et al. Stress-strain curves for steel fiber-reinforced concrete in compression. Revista Materia. 2010;15(2):260-6.
[33] Ou YC, Tsai MS, Liu KY, Chang KC. Compressive behavior of steel-fiber-reinforced concrete with a high reinforcing index. J Mater Civ Eng. 2012;24(2):207-15.
[34] Sabariman B, Soehardjono A, Wisnumurti, Wibowo A, Tavio. Stress-strain behavior of steel fiber-reinforced concrete cylinders spirally confined with steel bars. Adv Civ Eng. 2018;2018(1):1-8.

[35] Sabariman B, Soehardjono A, Wisnumurti, Wibowo A, Tavio. Stress-strain model for confined fiber-reinforced concrete under axial compression. Arch Civ Eng. 2020;66(2):119-133.

[36] Shakya K, Watanabe K, Matsumoto K, Niwa J. Application of steel fibers in beam-column joints of rigid-framed railway bridges to reduce longitudinal and shear rebars. Constr Build Mater. 2012;27(1):482-9.

[37] Eltobgy HH. Structural design of steel fiber reinforced concrete in-filled steel circular columns. Steel Compos Struct. 2013;14(3):267-82.

[38] Christianto D, Tavio, Kurniadi D. Effect of steel fiber on the shear strength of reactive powder concrete. IOP Conf Ser: Mater Sci Eng. 2019;508:012006.

[39] Nurdiansyah N. Mix proportion data sheet atoz mix instant (Form: MPA-4C). Jakarta: Albicon Reka Sarana; 2024.

[40] Rudnicki T, Stałowski P. Fast-setting concrete for repairing cement concrete pavement. Materials. 2023;16(17):5909.

[41] Yi ST, Kim JK, Oh TK. Effect of strength and age on the stress-strain curves of concrete specimens. Cem Concr Res. 2003;33(8):1235-44.

[42] ACI. ACI 318M-19: Building code requirements for structural concrete and commentary. USA: American Concrete Institute; 2019.

[43] Tavio, Machmoed SP, Raka IGP. Behavior of square RC columns confined with interlocking square spiral under axial compressive loading. Int J Eng Appl. 2022;10(5):322-35.